High-Frequency CMUT Arrays for High-Resolution Medical Imaging

Ömer Oralkan, Sean T. Hansen, Barış Bayram, Göksen G. Yaralıoğlu, A. Sanlı Ergun, and Butrus T. Khuri-Yakub
E. L. Ginzton Laboratory
Stanford University
Stanford, CA 94305-4088, U.S.A.

Abstract— **This paper describes high-frequency 1-D CMUT arrays designed and fabricated for use in electronically scanned high-resolution ultrasonic imaging systems. Two different designs of 64-element linear CMUT arrays are presented in this paper. A single element in each array is connected to a single-channel custom front-end integrated circuit for pulse-echo operation. The first design has a resonant frequency of 43 MHz in air, and operates at 30 MHz in immersion. The second design exhibits a resonant frequency of 60 MHz in air, and operates at 45 MHz in immersion. The experimental results are compared to simulation results obtained from the equivalent circuit model and nonlinear dynamic finite element analysis; a good agreement is observed between these results. This paper also briefly discusses the effects of the area fill factor on the frequency characteristics of CMUTs, which reveals that the transducer active area should be maximized to obtain a wideband response at high frequencies.**

I. Introduction

Diagnostic ultrasonic imaging systems used in some clinical applications such as dermatology, ophthalmology and intravascular imaging, and in biological research such as small animal imaging require very high resolution [1]. Because these applications do not call for deep penetration, they allow the use of high-frequency ultrasound at safe acoustic power levels. These systems, operating in the frequency range greater than 20 MHz, are often designed using mechanically scanned single transducer elements with a fixed focus. Because of mechanical scanning, systems based on single transducers are limited in frame rate. These systems cannot achieve a uniform resolution, due to the use of a fixed focus transducer.

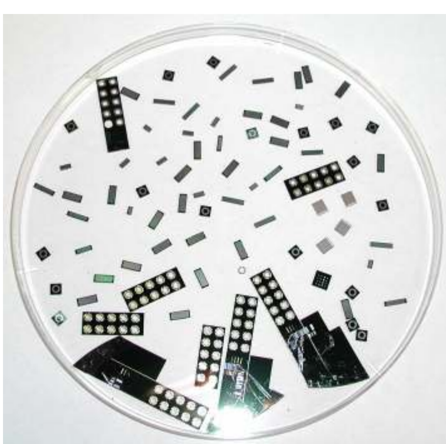

Fig. 1. CMUT arrays with different geometries and operating frequencies all fabricated on a single 4-inch silicon wafer.

In recent years, the design of high-frequency ultrasonic transducer arrays using both composite and non-composite piezoelectrics has been subject of significant research efforts [2, 3]. The vertical and lateral dimensions of transducer arrays should be scaled down for high frequency operation. The fabrication of these arrays involves meticulous and labor-intensive steps, such as hand lapping, high-precision dicing, and providing micro-interconnects. The efficiency and yield of these arrays are also considerably lower than large scale devices.

Capacitive micromachined ultrasonic transducer (CMUT) technology takes advantage of integrated circuit fabrication techniques to achieve the very small device dimensions required for high frequency operation. Basic microlithography and batch processing techniques allow thousands of arrays to be fabricated at a time on each run. Arrays with different operating frequencies, different numbers of elements, and even with different geometries, can be fabricated on a single silicon wafer. This approach results in uniform quality and reduced cost. Fig. 1 shows 1-D, 2-D and annular ring arrays, all fabricated on a single 4-inch silicon wafer. These transducers are inherently wideband, and provide sensitivity comparable to piezoelectric transducers [4, 5]. This technology also conveniently integrates the transducer array with supporting electronic circuits (either monolithically or in a flip-chip package) [6-8], which is especially critical for high-frequency applications, where parasitic components that are presented by interconnects could significantly degrade the overall system performance.

In this paper, we present two 64-element 1-D linear CMUT array designs and preliminary pulse-echo results obtained using a single channel custom integrated front-end ultrasonic transceiver wire-bonded to a single element of the array.

II. High-Frequency CMUT Arrays

We reported previously on high-frequency CMUTs designed as a single element for use alongside microfluidic channels on a lab-on-chip platform [9]. These transducers were tested using off-the-shelf electronic components; a frequency response centered around 45 MHz was demonstrated. This paper extends our previous work to arrays.

The high-frequency CMUT arrays presented in this paper are fabricated using the conventional surface micromachining process. The membrane and insulation layer materials are silicon nitride. Images of these CMUT arrays are shown in Fig. 2. The physical dimensions of the two designs subject to this work are summarized in Table I. The two designs differ

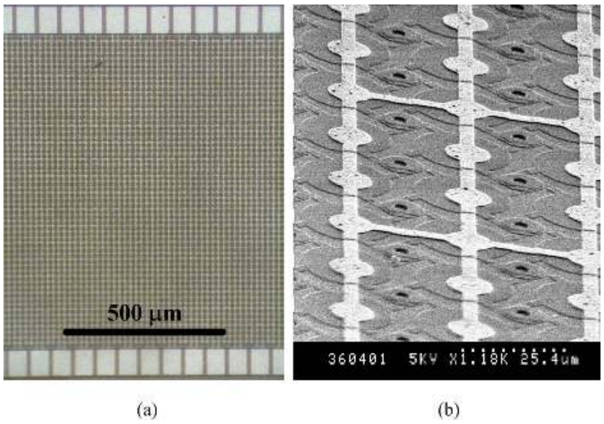

Fig. 2. (a) A group of elements in a high-frequency CMUT array. (b) A SEM photograph of a group of cells.

TABLE I. PHYSICAL PARAMETERS OF THE HIGH-FREQUENCY 1-D CMUT ARRAYS

	Design I	**Design II**
Length of an element, *µm*	1000	1000
Element pitch (d), *µm*	36	36
Number of cells per element	110	110
Cell radius (r_{cell}), *µm*	6	5
Electrode radius (r_{el}), *µm*	4	3
Cell center spacing (d_{cell}), *µm*	18	18
Metal electrode thickness (t_e), *µm*	0.3	0.3
Membrane thickness (t_m), *µm*	0.4	0.4
Gap thickness (t_g), *µm*	0.15	0.15
Insulating layer thickness (t_i), *µm*	0.08	0.08
Silicon substrate thickness, *µm*	500	500
Number of elements per array	64	64

from each other only in the cell and electrode radii. By following the same process flow both designs can be fabricated on the same wafer.

III. EXPERIMENTAL WORK

We performed impedance measurements and pulse-echo tests to characterize the transducer arrays. Using a vector network analyzer (model 8751A, Hewlett-Packard Co., Palo Alto, CA), we measured the electrical input impedance of a single element from each array in air. Both arrays were biased at 100 V and operated in the conventional regime. The electrical input impedance of a single transducer array element is shown in Fig. 3 for both design I and design II, along with simulation results obtained from the equivalent circuit model of the transducer. The resonant frequency in air is 43 MHz for design I, and 60 MHz for design II. The respective device capacitances are 0.22 pF and 0.12 pF. The parasitic capacitance for this particular measurement setup is around 1.3 pF.

For pulse-echo measurements, we placed the 64-element 1-D linear CMUT array into the cavity of a standard DIP-16 package, along with the front-end IC that comprises a pulse driver, a T/R switch, a wideband low-noise preamplifier, and an output buffer to drive off-chip loads. This circuit was fabricated in a standard 0.25-µm standard CMOS process, with

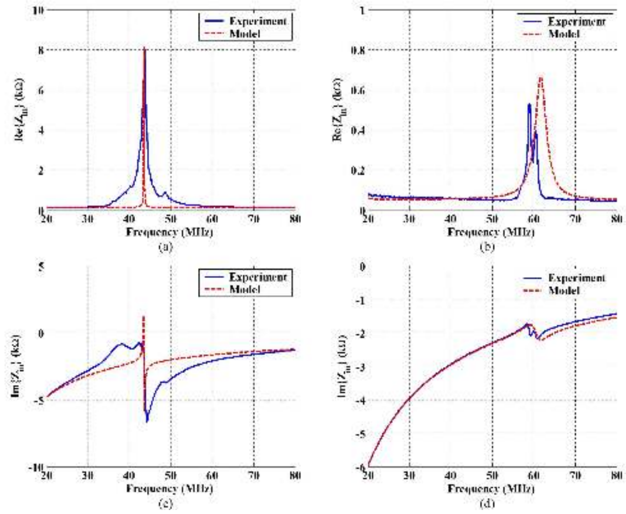

Fig. 3. Experimental results and equivalent circuit model simulations for the electrical input impedance: (a) Design I, real part, (b) design II, real part, (c) design I, imaginary part, (d) design II, imaginary part.

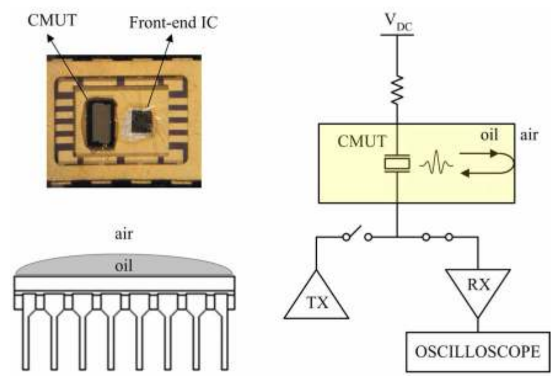

Fig. 4. Experimental pulse-echo setup.

a 2.5-V nominal supply voltage, and occupies an active silicon area of 70-µm x 70-µm. The electrical connections between a single element, the front-end IC and the package pins were provided by wire bonding. A photograph of the package is shown in Fig. 4(a). The CMUT array was immersed in vegetable oil, so that an oil-air interface was formed 0.5-1 mm away from the transducer, as shown in Fig. 4(b). The transducers were biased using a high-voltage DC power supply (model PS310 Stanford Research Systems, Inc., Sunnyvale, CA) at 100 V, and a 5-V unipolar pulse with variable width was used for excitation. The received echo signals were sampled at a rate of 1 GSa/s and digitized with an 8-bit resolution by a digitizing oscilloscope (model 54825A, Hewlett-Packard Co., Palo Alto, CA). A schematic representation of the experimental setup is shown in Fig. 4(c).

The received echo signals and corresponding Fourier transforms for designs I and II are shown in Fig. 5(a),(d) and (g),(j), respectively. The pulse width was 16 ns and 12 ns for designs I and II, respectively. In immersion, the operating frequencies for design I and II shift to 30 MHz and 45 MHz, respectively, and the response becomes wideband, due to the

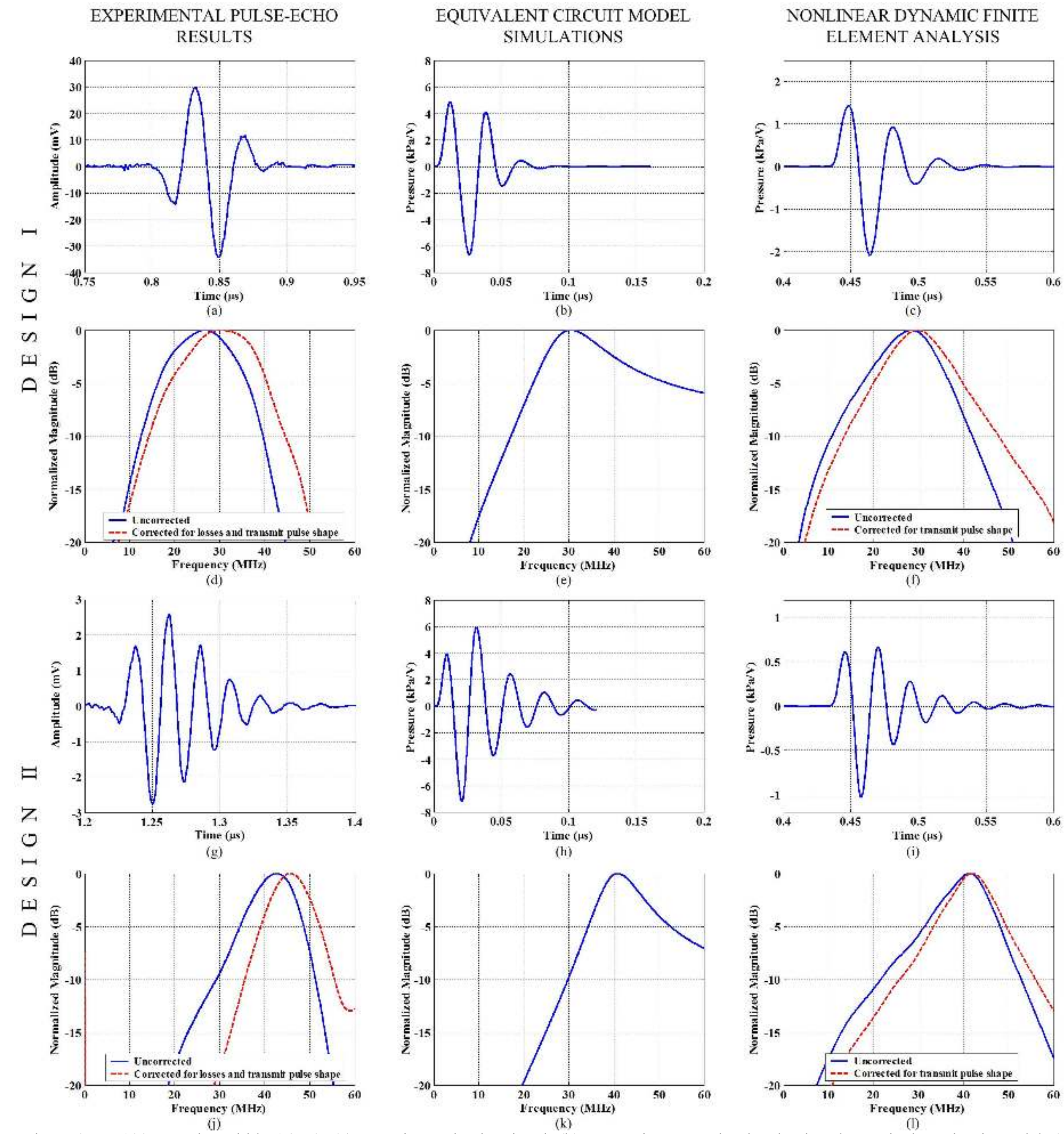

Fig 5. Design I (V_{DC}=100 V, pulse width=16 ns): (a) Experimental echo signal, (b) Transmit output simulated using the equivalent circuit model, (c) Transmit output simulated using nonlinear dynamic finite element analysis. (d) Experimental pulse-echo frequency spectrum, (e) Frequency spectrum simulated using the equivalent circuit model (f) Frequency spectrum simulated using nonlinear dynamic finite element analysis; Design II (V_{DC}=100 V, pulse width=12 ns): (g) Experimental echo signal, (h) Transmit output simulated using the equivalent circuit model, (i) Transmit output simulated using nonlinear dynamic finite element analysis. (j) Experimental pulse-echo frequency spectrum, (k) Frequency spectrum simulated using the equivalent circuit model (l) Frequency spectrum simulated using nonlinear dynamic finite element analysis.

TABLE II. COMPARISON OF EXPERIMENTAL AND SIMULATED FREQUENCY CHARACTERISTICS

Design	V_{DC}	Excitation	Operation Regime	Experimental Pulse-Echo Results		Equivalent Circuit Model Transmit Simulations		Nonlinear Dynamic FEA in Transmit	
				f_0	6-dB BW	f_0	3-dB BW	f_0	3-dB BW
I	100 V	-5 V, 16 ns	conventional	29.5 MHz	23.6 MHz	33 MHz	17.5 MHz	29.9 MHz	14.2 MHz
II	100 V	-5 V, 12 ns	conventional	45.6 MHz	14.6 MHz	42 MHz	11.7 MHz	41.7 MHz	11.2 MHz

fluid mass loading. These experimental results are compared to simulation results obtained from the equivalent circuit model [Fig. 5 (b),(e),(h), and (k)], and to the results of nonlinear transient dynamic finite element analysis [Fig. 5 (c),(f),(i),

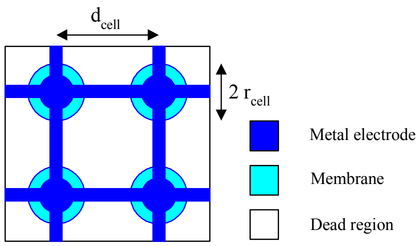

Fig. 6. A schematic definition of transducer fill factor.

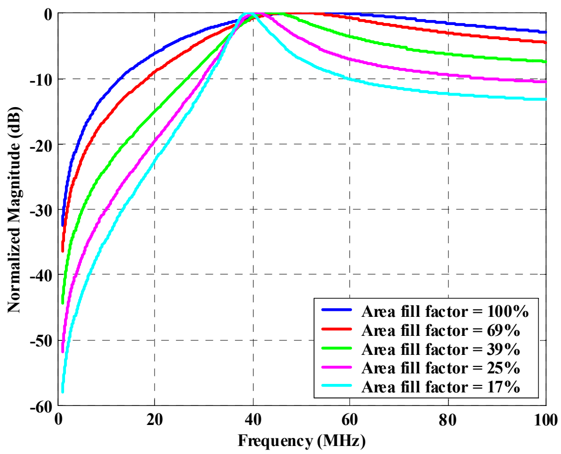

Fig. 7. Frequency response as a function of fill factor.

TABLE III. EFFECT OF FILL FACTOR ON THE FREQUENCY CHARACTERISTICS

r_{cell} (µm)	Fill Factor	f_0 (MHz)	3-dB Bandwidth (MHz)	Fractional Bandwidth
5	100%	65	72	111%
5	69%	56	46	82%
5	39%	47	21	45%
5	25%	42	12	29%
5	17%	40	8	20%

and (l)] [10]. The measurements on the experimental and simulated results are summarized in Table II. The 6-dB bandwidth is listed for the pulse-echo experimental results; the 3-dB bandwidth is used for transmit-only simulation cases. The experimental frequency characteristics are in good agreement with the simulated results.

Compared to measurements reported on CMUTs to date, the frequency response of these arrays showed a relatively narrow bandwidth. After investigating this unusual behavior in CMUT frequency response, we concluded that this effect is a result of low fill factor (25% for design II). The fill factor is defined as the ratio of the active area of a transducer to its total area (Fig. 6). The effective radiation impedance changes as a function of the fill factor. When the fill factor is low, each membrane acts more like an individual element by pushing the fluid sideways as well as in the normal direction. The hydrodynamic mass of the fluid increases, which leads to lower center frequency and reduced bandwidth. The equivalent circuit model used in this study accounts for this effect [11], and predicts that by increasing the fill factor and designing the membrane appropriately, wideband CMUTs can be designed at high frequencies (Fig. 7, Table III).

IV. CONCLUSION

The preliminary results presented in this paper show that high-frequency CMUT arrays can be designed and fabricated easily. These arrays, combined with custom integrated front-end circuits, demonstrate excellent signal quality at no loss in bandwidth. With all its cost and performance advantages, CMUT technology offers an excellent approach for the implementation of high-resolution medical and biological imaging systems. The operating frequency can be further increased by this technology to enable an electronically scanned acoustic microscope.

ACKNOWLEDGMENT

This work was supported by the National Institutes of Health. The authors would like to thank National Semiconductor Corporation for the fabrication of the prototype front-end integrated circuits.

REFERENCES

[1] G. R. Lockwood, D. H. Turnbull, D. A. Christopher, and F. S. Foster, "Beyond 30 MHz [Applications of high-frequency ultrasound imaging]," *IEEE Eng. Med. Biol. Mag.*, vol. 15, no. 6, pp. 60-71, Nov.-Dec. 1996.

[2] A. Nguyen-Dinh et al., "High-frequency piezo-composite transducer array designed for ultrasound scanning application," in *Proc. IEEE Ultrason. Symp.*, 1996, pp. 943-946.

[3] T. A. Ritter, T. R. Shrout, and K. K. Shung, "Development of high-frequency medical ultrasound arrays," in *Proc. IEEE Ultrason. Symp.*, 2001, pp. 1127-1133.

[4] Ö. Oralkan, X. C. Jin, F. L. Degertekin, and B. T. Khuri-Yakub, "Simulation and Experimental Characterization of a 2-D Capacitive Micromachined Ultrasonic Transducer Array Element," *IEEE Trans. Ultrason., Ferroelect., Freq. Cont.*, vol. 46, no.6, pp. 1337-1340, Nov. 1999.

[5] Ö. Oralkan et al., "Capacitive micromachined ultrasonic transducers: Next-generation arrays for acoustic imaging?," *IEEE Trans. Ultrason., Ferroelect., Freq. Cont.*, vol. 49, no. 11, pp. 1596-1610, Nov. 2002.

[6] Ö. Oralkan et al., "Volumetric Ultrasound Imaging Using 2-D CMUT Arrays," *IEEE Trans. Ultrason., Ferroelect., Freq. Cont.*, vol. 50, no. 11, pp. 1581-1594, Nov. 2003.

[7] I. O. Wygant et al., "Integrated ultrasonic imaging systems based on CMUT arrays: Recent progress," presented at the IEEE Intl. Ultrason. Symp., Montreal, Canada, 2004.

[8] R. A. Noble et al., "A cost-effective and manufacturable route to the fabrication of high-density 2D micromachined ultrasonic transducer arrays and (CMOS) signal conditioning electronics on the same silicon substrate," in *Proc. IEEE Ultrason. Symp.*, 2001, pp. 941-944.

[9] H. Jagannathan, G. G. Yaralioglu, A. S. Ergun, F. L. Degertekin, and B. T. Khuri-Yakub, "Micro-fluidic channels with integrated ultrasonic transducers," in *Proc. IEEE Ultrason. Symp.*, 2001, pp. 859-862.

[10] B. Bayram, G. G. Yaralioglu, A. S. Ergun, Ö. Oralkan, and B. T. Khuri-Yakub, "Dynamic FEM analysis of multiple CMUT cells in immersion," presented at the IEEE Intl. Ultrason. Symp., Montreal, Canada, 2004.

[11] A. Lohfink, P.-C. Eccardt, W Benecke, and H. Meixner, "Derivation of a 1D CMUT model from FEM results for linear and nonlinear equivalent circuit simulation," in *Proc. IEEE Ultrason. Symp.*, 2003, pp. 465-468.